Published in final edited form as:
Ann Biomed Eng. 2010 August ; 38(8): 2499–2511. doi:10.1007/s10439-010-0023-5.

Permeability of Endothelial and Astrocyte Cocultures: *In Vitro* Blood–Brain Barrier Models for Drug Delivery Studies

Guanglei Li[1], **Melissa J. Simon**[2], **Limary M. Cancel**[1], **Zhong-Dong Shi**[1], **Xinying Ji**[1], **John M. Tarbell**[1], **Barclay Morrison III**[2], and **Bingmei M. Fu**[1]

[1]Department of Biomedical Engineering, The City College of the City University of New York, New York, NY 10031, USA

[2]Department of Biomedical Engineering, Columbia University, New York, NY 10027, USA

Abstract

The blood–brain barrier (BBB) is a major obstacle for drug delivery to the brain. To seek for *in vitro* BBB models that are more accessible than animals for investigating drug transport across the BBB, we compared four *in vitro* cultured cell models: endothelial monoculture (bEnd3 cell line), coculture of bEnd3 and primary rat astrocytes (coculture), coculture with collagen type I and IV mixture, and coculture with Matrigel. The expression of the BBB tight junction proteins in these *in vitro* models was assessed using RT-PCR and immunofluorescence. We also quantified the hydraulic conductivity (L_p), transendothelial electrical resistance (TER) and diffusive solute permeability (P) of these models to three solutes: TAMRA, Dextran 10K and Dextran 70K. Our results show that L_p and P of the endothelial monoculture and coculture models are not different from each other. Compared with *in vivo* permeability data from rat pial microvessels, P of the endothelial monoculture and coculture models are not significantly different from *in vivo* data for Dextran 70K, but they are 2–4 times higher for TAMRA and Dextran 10K. This suggests that the endothelial monoculture and all of the coculture models are fairly good models for studying the transport of relatively large solutes across the BBB.

Keywords

In vitro blood–brain barrier; bEnd3; Astrocyte; Coculture; Hydraulic conductivity; Diffusive solute permeability; Expression of junction proteins

INTRODUCTION

The blood–brain barrier (BBB) is an interface between the blood circulation and the central nervous system (CNS). Its unique structural characteristics make it minimally permeable to water and solutes, which is essential for the normal function of the CNS. Endothelial cells line the luminal surface of the cerebral microvessel and, at the abluminal side of the endothelial cells, there is a complete wrapping of the basement membrane (BM), 99% of

Address correspondence to Bingmei M. Fu, Department of Biomedical Engineering, The City College of the City University of New York, New York, NY 10031, USA. fu@ccny.cuny.edu.

which is covered by astrocyte foot processes. The close apposition of astrocytes to endothelial cells is thought to be necessary for the development and maintenance of the BBB junction proteins.[1,19,21] The uniform and thin matrixlike BM sandwiched between the astrocytes and the endothelium consists of collagen type IV, heparin sulfate proteoglycans, laminin, fibronectin, and other extracellular matrix (ECM) proteins.[25,29,30,34] It acts as a permeability barrier, retarding the movement of molecules into brain tissue, and participates in the maintenance of the BBB integrity.[20] The tight junctions and adherens junctions between adjacent endothelial cells of the BBB form tighter seals than those of their peripheral counterparts. These junction complexes consist of transmembrane proteins, e.g., occludin, claudin, junction adhesion molecules, and vascular endothelial (VE)-cadherin.[20] The transmem-brane proteins are linked to the actin cytoskeleton of the endothelium via accessory proteins such as members of the zonula occludens family, ZO-1, ZO-2 and ZO-3.[31]

To investigate the mechanisms by which the BBB maintains and regulates its permeability in health and disease, various *in vivo* and *in vitro* models have been used to study transport across the BBB. *In vitro* BBB models have been widely used due to their low cost, repeatability, and feasibility in performing high-throughput screening and investigating regulatory mechanisms at the molecular level, despite losing some expression of the BBB efflux protein systems and having a comparatively higher permeability compared to *in vivo* models.[35] The cells for these *in vitro* models are obtained either from primary/sub-passaged or immortalized cell cultures. Primary brain capillary endothelial cells have the closest resemblance to the BBB phenotype *in vivo* and exhibit excellent characteristics of the BBB at early passages.[35] They, however, have inherent disadvantages such as being extremely time consuming and costly to generate, being easily contaminated by other neurovascular unit cells, losing their BBB characteristics over passages, and requiring high technical skills for extraction from brain tissue.[6,11] An immortalized mouse brain endothelial cell line, bEnd3, has recently been under investigation for *in vitro* BBB models because of its numerous advantages over primary cell culture: the ability to maintain BBB characteristics over many passages, easy growth and low cost, formation of functional barriers and amenability to numerous molecular interventions.[6,43,46,50,51] Previous RT-PCR analysis showed that bEnd3 cells express the tight junction proteins ZO-1, ZO-2, occludin and claudin-5, and junctional adhesion molecules.[6,36] They also maintained functionality of the sodium- and insulin-dependent stereospecific facilitative transporter GLUT-1 and the P-glycoprotein efflux mechanism,[36] formed fairly tight barriers to radiolabeled sucrose, and responded like primary cultures to disrupting stimuli.[6]

To characterize the transport properties of *in vitro* BBB models, Malina *et al.*.[32] and others[2,3,18,23,24,27,38,40,45] measured the diffusive permeability of endothelial cell monolayer and coculture of endothelial cells with as-trocyctes to fluorescence or isotope labeled tracers, e.g., sucrose, inulin, and mannitol. Sahagun *et al.*.[39] reported the ratio between abluminal concentration and luminal concentration of different-sized dextrans (4k, 10k, 20k, 40k, 70k, and 150k) across mouse brain endothelial cells. Gaillard and de Boer[16] measured the permeability of sodium fluorescein and FITC-labeled Dextran 4k across a coculture of calf brain capillary endothelial cells with rat astrocytes. Many investigators have measured the

transendothelial electrical resistance (TER) of brain endothelial monolayers and cocultures as an indicator of ion permeability.[10,12,41,53]

To search for an effective, relatively convenient, and inexpensive *in vitro* BBB model, we characterized the junction protein expression and quantified the TER and permeability to water and solutes of four *in vitro* BBB models: bEnd3 monoculture, bEnd3 coculture with astrocytes, coculture with two BM substitutes: collagen type I and IV mixture, and Matrigel. Collagen type IV network is the basic framework of native BM[13,34] and Matrigel is a soluble and sterile extract of BM derived from the EHS tumor, which has been widely used as a reconstituted BM in studying cell morphogenesis, differentiation and growth.[25] As negative controls, we also characterized the transport properties of astrocyte monoculture and astrocyte monoculture with Matrigel coating.

MATERIALS AND METHODS

Cell Culture

Immortalized mouse endothelial cells, bEnd3, from American Type Culture Collection (Manassas, VA) were cultured in Dulbecco's modified Eagle's medium (DMEM) (Sigma, St. Louis, MO) with 10% fetal bovine serum (FBS) (Hyclone, Logan, UT), 3 mM L-glutamine (Sigma, St. Louis, MO) and 1% penicillin–streptomycin (PS) (Sigma, St. Louis, MO). Cells (passage 15–30) were maintained in a humidified cell culture incubator at 37 °C and with 5% CO_2/95% air.

The astrocytes were obtained from the cortices of 8- to 10-day-old Sprague–Dawley rat pups. All procedures involving animals were approved by the Columbia University IACUC. Briefly, the brain was removed and placed into a Petri dish containing a few drops of salt solution. The cortex was separated, minced, and digested in papain (Sigma, St. Louis, MO) for 30 min at 32 °C. The digested tissue was triturated and transferred to a T75 flask containing Neurobasal-A medium with 5% B27 supplement (Invitrogen, Carlsbad, CA), 1 mM glutamine and 5 mg/mL D-glucose (Sigma, St. Louis, MO). After an hour, the flasks were vigorously shaken and the media was discarded. The remaining astrocytes were grown in DMEM with 10% fetal bovine serum, 1 mM glutamine, and 1% PS for 2 weeks. The media in the flask was replaced every two days.

For astrocyte and bEnd3 monocultures, the Trans-well filters (0.4-μm pore size, 12-well; Corning, Lowell, MA) were coated with fibronectin (30 μg/mL). Astrocytes were seeded onto the abluminal side of the filter at a density of 2.75×10^4 cells per filter and grown for 5–6 days. The bEnd3 cells were seeded onto the luminal side of the filter at a density of 6.6×10^4 cells per filter and grown for 3–4 days.

The procedure for coculturing bEnd3 cells and astrocytes is shown in Fig. 1. The Transwell filter was first coated with fibronectin or basement membrane substitutes (collagen type I and IV mixture or Matrigel) as described below. The Transwell filter was then inverted and astrocytes were seeded onto the abluminal side of the filter at a density of 2.75×10^4 cells per filter and allowed to adhere for 2 h. After that, the filter was flipped back and astrocytes were cultured in DMEM with 10% FBS and 1% PS for 2 days. At the end of 2 days, bEnd3

cells were seeded onto the luminal side of the filter at a density of 6.6×10^4 cells per filter and cocultured with astrocytes for an additional 3–4 days. The medium from both luminal and abluminal sides of the Transwell filter was changed every other day.

Basement Membrane Coating

We used Matrigel and a mixture of collagen types I and IV as the basement membrane substitutes for our *in vitro* BBB models. For Matrigel coating, Matrigel (BD Biosciences, Bedford, MA) was diluted in Dulbecco's PBS (DPBS; Mediatech, Herndon, VA) to a concentration of 476 μg/mL. The Transwell filter was reversed and 200 μL of diluted Matrigel solution was added to the abluminal side of each Transwell filter. The Transwell plate containing the filters was placed in a 37 °C, 5% CO_2−95% air incubator for 3 h for the Matrigel to gel. For collagen mixture coating, types I and IV collagen (BD Bioscience, Bedford, MA) were diluted in DPBS to 0.5 mg/mL and their pH brought to 7.4 with NaOH and HCl respectively. The two collagens were then mixed thoroughly (40:60, collagen I: collagen IV, v/v) and 200 μL of the mixture was added to the luminal side of each Transwell filter. The Transwell plates with filters were incubated at 37 °C for 1 h for the mixture to gel. After that, the Matrigel and collagen mixture coated Transwell filters were placed into a sterile hood and allowed to air dry for 24–72 h. Once dry, filters were stored at 4–8 °C for up to 2 weeks. The coated filters were rehydrated in DPBS for 1 h in a 37 °C, 5%CO_2−95% air incubator prior to cell seeding.

Immunostaining of Junction Proteins

Astrocytes and bEnd3 cells were grown on Transwell filters as described above. For staining astrocytes, the cells were washed 3× with DPBS, fixed in 3.7% formaldehyde for 15 min, washed 3× with DPBS, permeabilized with 0.1% Triton X-100 in DPBS for 10 min and then blocked with 5% horse serum (Sigma, St. Louis, MO) in DPBS for 30 min. The astrocytes were then incubated with rabbit anti-glial fibrillary acidic protein (GFAP, Sigma, St. Louis, MO) overnight at room temperature. The astrocytes were then washed 3× with DPBS and incubated with Alexa Fluor 594 goat anti-rabbit secondary antibody (1:200; Invitrogen, Carlsbad, CA) for 1 h at room temperature. For nucleus couterstaining, the astrocytes were incubated in 4′,6-diamidino-2-phenylindole (DAPI, 1:500; Invitrogen, Carlsbad, CA) for 15 min at room temperature. For cytoplasm staining, separate unfixed astrocyte monolayers were washed 3× with DPBS and then incubated in Calcein AM (1:500; Invitrogen, Carlsbad, CA) for 15 min at 37 °C.

For immunostaining bEnd3 cells, monocultures or cocultures were washed 2× with DPBS, fixed in 1% paraformaldehyde for 10 min, permeabilized with 0.2% Triton X-100 in DPBS for 10 min and blocked with 10% bovine serum albumin (BSA) and 0.1% Triton X-100 in DPBS for 1 h. After washing with DPBS, the monolayers were incubated with a primary antibody for claudin-5, occludin, ZO-1 or VE-caherin (1:200; Zymed, San Francisco, CA) for 3 h at room temperature or overnight at 4 °C. The cell monolayers were then washed 5× with DPBS and incubated with an Alexa Fluor 488 donkey anti-rabbit IgG secondary antibody (1:200; Invitrogen, Carlsbad, CA) for 1 h at room temperature. The nuclei were counterstained by incubating with propidium iodide (PI, 1:1000; Invitrogen, Carlsbad, CA) for 15 min.

Immunostained cells were observed with a Nikon Eclipse TE2000-E microscope. Images were taken with a Photometrics Cascade 650 CCD camera from Roper Scientific (Tucson, AZ).

RNA Extraction and Gene Expression Analysis

Total RNA was isolated from bEnd3 cells using TRIzol LS reagent (Invitrogen, Carlsbad, CA) and quantitative reverse transcription-polymerase chain reaction (RT-qPCR) was conducted to analyze gene expression as previously described. RNA was first converted to cDNA, and then real-time PCR was performed on the ABI PRISM 7000 sequence detection system (Applied Biosystems, CA). β-Actin served as an internal control. The PCR reactions were performed in 25 μL reaction mixture volumes containing SYBR Green PCR Master Mix (Applied Biosystems), cDNA, and specific primer pairs. RT-qPCR programs were set to 15 min at 95 °C, followed by 40 cycles of 20 s at 95 °C, 30 s at 55 °C, and 30 s at 72 °C. The specificity of the amplification reaction was assessed by performing a dissociation curve analysis. Primer sequences are listed in Table 1.

Measurement of L_p and P

The hydraulic conductivity L_p and solute diffusivity P of the cell layers were measured using a previously developed bubble tracker system and automated fluorometer system as shown in Fig. 2.[7,8] Briefly, the Transwell filter containing cultured cell layers was sealed within a transport chamber to form luminal and abluminal compartments. The transport chamber was connected to a laser excitation source and an emission detector via optical fibers. The fluorescent tag of the test solute in the abluminal chamber was excited by the excitation light produced by a 10-mW Crystal laser and the emission was counted by a photon counting detector. The data was recorded by the *FluoroMeasure* acquisition software (C&L Instruments, Hummelstown, PA). The abluminal compartment of the transport chamber was also connected to a water reservoir by a Tygon and borosilicate glass tube as shown in Fig. 2. A hydrostatic pressure difference could be created across the filters by adjusting the height of the reservoir with respect to the height of the fluid covering the cell layers. Water flux across the cell layers was measured by tracking the position of a bubble pre-inserted into the glass tube. Both the luminal compartment and abluminal reservoir were continuously supplied with 5% CO_2−95% air to maintain the pH of the medium at 7.4. The temperature of the whole permeability measurement system was maintained at 37 °C.

Before the transport experiment, the abluminal compartment of the chamber was filled with the experimental medium (1% bovine serum albumin and 1% Penicillin/Streptomycin in DMEM medium free of phenol red). The Transwell filter with the cell layer was rinsed twice with the experimental medium and then sealed in the transport chamber. A high concentration of test solute with fluorescent tag was added to the luminal compartment of the chamber. Each experiment lasted 3 h: the first hour for equilibration, the second hour for data collection under convective condition ($\Delta p = 10$ cmH_2O), and the final hour of data collection under diffusive conditions ($\Delta p = 0$).

Calculation of L_p and P

During the second hour of the transport experiments, the reservoir was lowered by 10 cm, thus applying a hydraulic pressure difference of 10 cmH_2O across the cell layer. To measure the volumetric flow rate (J_v), the air bubble displacement was tracked and converted to J_v according to the following equation

$$J_v=(\Delta d/\Delta t)\times F \quad (1)$$

where $\Delta d/\Delta t$ is the bubble displacement rate and F is a tube calibration factor (fluid volume occupying a known length of tubing). Because the upper and lower chambers contained the same medium (DMEM with 1% BSA), there was no osmotic pressure difference across the cell layer. The hydraulic conductivity L_p was thus calculated as

$$L_p=J_v/A/\Delta p \quad (2)$$

where A is the surface area of the Transwell filter (1.1 cm^2) and Δp is the hydraulic pressure difference across the cell layer.

The fluorescence intensity in the abluminal compartment was recorded during the experiment and converted to concentration through a calibration curve. The solute flow across the cell layer (J_s) was calculated by the following equation

$$J_s=(\Delta C_a/\Delta t)\times V_a \quad (3)$$

where $\Delta C_a/\Delta t$ is the rate change of concentration in the lower chamber and V_a is the fluid volume in the lower compartment. The diffusive solute permeability (P) was then calculated by

$$P=J_s/A/(C_L-C_a)=J_s/A/C_L \quad (4)$$

where $C_L$is the solute concentration in the upper compartment and A is the surface area of the filter. The concentration in the lower chamber C_a was neglected in Eq. (4) because the solute concentration in the upper chamber, C_L, is much larger than C_a.

To calibrate the fluorometer system, ten different concentrations of test solute were made according to the test solute concentration in the abluminal compartment obtained during a typical experiment. The fluorescent intensity of 3 mL of each solution was measured for 20 min in each chamber. A linear regression of the concentration vs. average intensity data was used to create a calibration curve.

The L_p and P measurements included both the cell layers and the Tranwell insert. The Transwell insert itself also provides resistance to the transport of water and solutes, therefore we also measured the L_p and P of the Transwell insert to various-sized solutes. The final permeability results presented for the *in vitro* models were adjusted to account for the Transwell insert.

Measurement of Transendothelial Electrical Resistance (TER)

The TERs of the *in vitro* BBB models grown on the Transwell inserts were recorded using an End-ohm chamber connected to an EVOM resistance meter (World Precision Inst. Inc., Sarasota, FL). TER of each model was calculated after subtracting the TER of the blank Transwell filters and reported as $\Omega\ cm^2$.

Statistical Analysis

The L_p and P are presented as mean ± SD. Data were analyzed for statistical significance by ANOVA with $p < 0.05$ being considered statistically significant.

RESULTS

Immunostaining of Astrocytes

The astrocytes used in our *in vitro* BBB models were isolated from 8- to 10-day-old rats. Since brain tissue contains many other cell types such as neurons, endothelial cells, and glial cells, it was important to examine the purity of the primary astrocyte cultures. Astrocytes were immunolabeled with an antibody against GFAP (red) as shown in Fig. 3a, and counterstained with cell nucleus dye DAPI (blue). Since DAPI stains the nuclei of all cell types while GFAP is only specific to astrocytes, the purity of astrocytes could be determined by matching the astrocyte body with the corresponding cell nucleus. As shown in Fig. 3a, the percentage of astrocytes was higher than 90%. For the transport experiments, it was required that the cells formed a confluent monolayer on the Transwell filter. Figures 3b and 3c demonstrate the fluorescence labeling of cytoplasm and GFAP of astrocytes both in monoculture and in coculture with bEnd3 cells, respectively. Astrocytes formed a fairly complete cell layer in both cases. Due to the special morphology of astrocytes, in some regions astrocyte foot processes were on top of other cell bodies so that the astrocyte monolayer was not as flat and compact as the endothelial monolayer.

Protein and Gene Expressions of bEnd3 Monolayer and Coculture

The expression of various junction proteins in our *in vitro* BBB models was examined by immunostaining. Figure 4 shows images of the tight junction transmembrane protein claudin-5 (Figs. 4a and 4b), occludin (Figs. 4c and 4d), accessory protein ZO-1 (Figs. 4e and 4f), and adherens junction transmembrane protein VE-cadherin (Figs. 4g and 4h). The left column shows staining of the bEnd3 monolayer alone, while the right column shows bEnd3 cells cocultured with astrocytes. In both cases, the bEnd3 cells formed confluent monolayers on the luminal side of the Transwell filter. Coculture with astrocytes did not alter the expression of claudin-5, occludin, ZO-1, and VE-cadherin of endothelial cells.

The gene expression of various junction proteins in the bEnd3 monocultures and cocultures is shown in Fig. 5. RNA was isolated from the confluent bEnd3 cell layer grown on the Transwell filter and the RT-qPCR was performed for claudin-5, occludin, ZO-1, VE-cadherin, and β-actin (internal control). The empty and filled bars show the results for the bEnd3 monolayer and the bEnd3 layer cocultured with astrocytes, respectively. As shown in Fig. 5, there was no significant difference in the mRNA level of all four junctional proteins between the bEnd3 monoculture and coculture, though the mRNA level for each of the

proteins was slightly increased when the bEnd3 cells were cocultured with astrocytes ($p > 0.2$). These results indicate that there was no dramatic change in the expression of junction protein components when bEnd3 cells were exposed to astrocytes for 3–4 days. The gene expression result was consistent with the observation of junction protein expression by immunostaining.

Hydraulic Conductivity (L_p) of In Vitro BBB Models

Figure 6 shows the measured hydraulic conductivity (L_p) of the *in vitro* BBB models: astrocyte monoculture and astrocyte monoculture on top of Matrigel (Astrocyte + Matrigel) as negative controls; bEnd3 monoculture; coculture of astrocytes and bEnd3 on different sides of the Transwell filter (coculture); coculture with the collagen type I and IV mixture (coculture + collagen mixture) and coculture with the Matrigel (coculture + Matrigel) coating on the luminal side of the Transwell filter. L_p of astrocyte monoculture was $5.0 \pm 2.7 \times 10^{-7}$ ($n = 15$) cm/s/ cmH_2O, which was slightly lower than that of the astrocyte monoculture with Matrigel, $5.1 \pm 2.9 \times 10^{-7}$ ($n = 10$) cm/s/cmH_2O. L_p of bEnd3 monoculture was $1.7 \pm 1.1 \times 10^{-7}$ ($n = 15$) cm/s/cmH2O, which was ~1/3 of that of the astrocyte monoculture with or without Matrigel coating ($p < 0.01$). The L_p of the coculture of bEnd3 with astrocytes was $1.4 \pm 0.6 \times 10^{-7}$ ($n = 16$) cm/s/cmH_2O, ~18% lower than that of bEnd3 monoculture, but not significantly different ($p = 0.13$). Coating with a mixture of collagen types I and IV decreased the L_p of the cocultures to $1.1 \pm 0.9 \times 10^{-7}$ ($n = 10$) cm/s/cmH_2O but not significantly ($p = 0.07$), while coating with Matrigel insignificantly increased the L_p of cocultures to $1.6 \pm 0.8 \times 10^{-7}$ ($n = 8$) cm/s/cmH2O ($p = 0.45$). These results suggest that bEnd3 cells provide the majority of the resistance to water transport in our *in vitro* BBB models.

Diffusive Permeability (P) of In Vitro BBB Models to Different-Sized Solutes

Figure 7 shows the measured diffusive permeability (P) of the *in vitro* BBB models to three different-sized solutes: (a) TAMRA (MW = 467), (b) Dextran 10K and (c) Dextran 70K. P^{TAMRA}, P^{Dex10k} and P^{Dex70k} of the astrocyte monoculture were 30.9 ± 18.7 ($n = 10$), 4.1 ± 1.2 ($n = 12$), and 0.9 ± 0.4 ($n = 12$) $\times 10^{-6}$ cm/s, respectively. Coating with Matrigel insignificantly increased P^{TAMRA}, P^{Dex10k}, and P^{Dex70k} of the astrocyte monoculture to 31.5 ± 12.5 ($n = 8$), 4.5 ± 1.7 ($n = 11$), and 1.2 ± 0.4 ($n = 16$) $\times 10^{-6}$ cm/s ($p > 0.11$), respectively. P^{TAMRA}, P^{Dex10k}, and P^{Dex70} of bEnd3 monoculture were 8.1 ± 3.6 ($n = 7$), 1.0 ± 0.45 ($n = 15$) and 0.21 ± 0.07 ($n = 15$) $\times 10^{-6}$ cm/s, respectively, which were 18–26% lower than those of the astrocyte monoculture with or without Matrigel coating ($p < 0.02$). P^{TAMRA}, P^{Dex10k}, and P^{Dex70} of the coculture of bEnd3 with astrocytes were 5.9 ± 1.9 ($n = 10$), 0.78 ± 0.24 ($n = 10$) and 0.16 ± 0.09 ($n = 11$) $\times 10^{-6}$ cm/s, respectively, which were 20–27% lower than those of the bEnd3 monoculture, but this difference was not significant ($p > 0.13$). Coating with the mixture of collagen types I and IV insignificantly decreased P^{TAMRA}, P^{Dex10k}, and P^{Dex70k} of the coculture to 5.8 ± 2.2 ($n = 8$), 0.67 ± 0.24 ($n = 12$) and 0.16 ± 0.09 ($n = 11$) $\times 10^{-6}$ cm/s, respectively ($p > 0.27$), while coating with Matrigel insignificantly increased P^{TAMRA}, P^{Dex10k}, and P^{Dex70k} of the coculture to 6.0 ± 2.5 ($n = 16$), 0.84 ± 0.20 ($n = 7$) and 0.17 ± 0.07(n= 13) $\times 10^{-6}$ cm/s, respectively ($p > 0.6$). These

results suggest that the endothelium of the *in vitro* BBB also provides the majority of the resistance to the transport of various-sized solutes.

Transendothelial Electrical Resistance (TER) of In Vitro BBB Models

We also measured the TER of our *in vitro* models. After culturing for 5 days, the astrocyte monolayer had a TER of 8.6 ± 3.2 (n = 3) Ωcm^2; the astrocyte monolayer on Matrigel had a lower TER of 4.0 ±1.8 (n = 4) Ωcm^2. After culturing or coculturing for 3–4 days, bEnd3 monolayers had a TER of 19.6 ± 2.7 (n = 7) Ωcm^2; coculture had a higher TER of 30.3 ± 6.4 (n = 6) Ωcm^2; coculture with collagen I and IV mixture had a TER of 24.2 ± 1.3 (n = 10) Ωcm^2 while coculture with Matrigel had a TER of 33.4 ± 2.8 (n = 3) Ωcm^2. Figure 8 shows the percent difference of the TER of each *in vitro* model compared to the bEnd3 monoculture. The TERs of the astrocyte monoculture and astrocyte monoculture on Matrigel were only 44% and 20% of the bEnd3, respectively ($p < 0.02$). However, coculture, coculture with collagen mixture and coculture with Matrigel had TERs that were 154%, 123% and 170% of the bEnd3 monolayer, respectively ($p < 0.01$).

DISCUSSION

In this study, we characterized four *in vitro* BBB models by examining the expression of junction proteins that characterize the endothelium and quantifying their permeability to water and solutes. The immortalized mouse brain microvessel endothelial cell line bEnd3 showed good expression of essential junction proteins: claudin-5, occludin, ZO-1, and VE-cadherin, while the primary rat astrocytes used in the coculture expressed GFAP.

Basement membrane (BM) is an important structural component of the BBB which has not been included in previous *in vitro* models of the BBB. In this work, two BM substitutes (Matrigel and collagen type I and IV mixture) were used and their effect on the transport properties of the BBB was examined. Although the major collagen existing in the native BM of the BBB is type IV,[25,29,30,34] we used a mixture of type I and IV (40:60, v/v) because collagen IV alone cannot form a gel. Among the tested *in vitro* models, the one with the collagen I and IV mixture had the lowest permeability, indicating that this mixture can enhance the integrity of the BBB. In contrast, the *in vitro* models with Matrigel had the highest permeability, suggesting that it is not a good BM for growing a tight BBB *in vitro*.

Astrocyte foot processes cover ~99% of the abluminal surface of cerebral microvessels *in vivo*.[37] The proximity of astrocytes to endothelial cells is thought to be important for the normal function of the BBB.[1] In this work, we examined the expression of the specific astrocytic protein, GFAP, and measured the permeability of an astrocyte monoculture, astrocyte monoculture with Matrigel, and astrocyte coculture with bEnd3 cells, and an astrocyte coculture with bEnd3 cells containing either a collagen I and IV mixture or Matrigel. Figures 6 and 7 indicate that astrocytes provide ~25% of total BBB resistance to water and ~20% of the resistance to various-sized solutes. The endothelium provides ~75–80% of the *in vitro* BBB resistance.

Among the tested *in vitro* BBB models, the coculture of bEnd3 cells and astrocytes with the collagen I and IV mixture had the lowest permeability to water and solutes, although there

was no significant difference between the coculture and the bEnd3 monoculture. Figure 9 shows a comparison of our measured diffusive solute permeabilities (*P*) with *in vivo* data from rat pial microvessels from Yuan *et al..*,[52] and data from an *in vitro* coculture model from Gaillard and Boer that used bovine brain capillary endothelial cells and rat astrocytes.[16] *P* was plotted as a function of the Stokes radius of the solutes. The Stokes radii for all the solutes except Dextran 70K were calculated using the Stokes–Einstein Equation based on their measured diffusion coefficients in the aqueous solution.[4,5,28,44] The Stokes radius of Dextran 70K was estimated from that of albumin with similar molecular weight.[52] The measured *P* of our bEnd3 monoculture, coculture, and coculture with collagen mixture to TAMRA, Dextrans 10K and 70K in our current study are represented by triangles, open circles and diamonds, respectively. The open squares represent data for NaF and Dextran 4K from Gaillard and Boer.[16] The *in vivo* data for NaF, Dextrans 4K, 10K, 20K, 40K, and 70K are represented by solid circles. For all three *in vitro* BBB models with bEnd3, the permeability to TAMRA and Dextran 10K is 2.4–3.3 and 2.6–3.8 times those of *in vivo* pial microvessels ($p < 0.005$), respectively, while the permeability to Dextran 70k is comparable to the *in vivo* data ($p > 0.2$). Our results indicate that the *in vitro* BBB models with bEnd3 cells are fairly good models for the transport of relatively large solutes across the BBB. Figure 9 also shows that our *in vitro* models using bEnd3 cells and primary rat astrocytes have comparable permeabilities to small solutes as the previous coculture model using bovine brain capillary endothelial cells and rat astrocytes.

Fraser *et al.*.[15] measured an L_p of 2.0×10^{-9} cm/s/ cmH_2O in frog pial microvessels *in vivo*. Compared with this *in vivo* data, L_p of all the *in vitro* BBB models are two orders of magnitude higher, indicating that our current *in vitro* models may not be ideal for water transport.

Although the TER of the bEnd3 monoculture is much smaller than ~1800 Ωcm^2, the *in vivo* value for rat cerebral microvessels,[9,11,17,32,41] the cocultures can increase the TER by up to 170% of that of the bEnd3 monoculture. Fletcher *et al.*.[14] developed *in vitro* BBB models using primary feline brain capillary endothelial cell monocultures and cocultures with astrocytes. The TERs of their monocultures and cocultures were 20–25 Ωcm^2 and 30–35 Ωcm^2 respectively, which are comparable to our data. Koto *et al.*.[26] measured the TER of a bEnd3 monoculture from 1 to 11 days after confluence (or 3–13 days after cell seeding). They found that the TER increased with days of culture, reaching the maximum of ~110 Ωcm^2 at day 8, and decreased afterwards. However, we observed that culturing for more than 3 days after confluence (or 5 days after cell seeding) resulted in obvious cell overgrowth. Compared to the *in vivo* TER data, the bEnd3 monoculture and the coculture with bEnd3 cells and astrocytes on different sides of the filter are not ideal barrier models for ion transport. The porous membrane in the Transwell filter separating the bEnd3 cells and the primary astrocytes is ~10 microns thick, thus the direct contact between the two cell types was missing in our coculture models. This may be one of the reasons for the low TER of the current coculture models. Although coculture on opposite sides of the Transwell filter has resulted in TERs of up to 1650 Ωcm^2,[32] and the paracine effects of glia or glioma cells have been found to be important in the induction and maintenance of BBB phenotype,[36] a coculture model with direct contact of endothelial and glial cells like astrocytes is expected

to increase the transport barrier to water and small ions. In addition, using primary brain endothelial cells and primary astrocytes or other glial cells from the same species, as well as controlling the maturation time using different ECMs, may improve the TER and L_p. Furthermore, since the endothelium *in vivo* is constantly exposed to the blood flow, coculture of endothelial cells with glial cells under a dynamic flow condition should also increase the TER.[41]

In summary, we established and characterized four *in vitro* BBB models of either bEnd3 cultured alone, or cocultured together with astrocytes with or without basement membrane substitutes. Astrocytes alone or astrocytes with Matrigel are by no means a good barrier model for simulating transport across the BBB. Although both bEnd3 monocultures and cocultures had relatively high permeabilities to water and ions, they had solute permeabilities comparable to that of the *in vivo* BBB, especially to relatively large solutes. The models used in this study are abundantly available, reproducible, convenient and cost effective, and thus are well suited for pharmacological studies.

Acknowledgments

This work was supported in part by the Andrew Grove Foundation, the National Science Foundation CBET-0133775 and CBET-0754158, PSC-CUNY research award of the City University of New York, and the National Institutes of Health grant HL57093.

REFERENCES

1. Abbott NJ. Astrocyte-endothelial interactions and blood-brain barrier permeability. J. Anat. 2002; 200:629–638. [PubMed: 12162730]
2. Boveri M, Berezowski V, Price A, Slupek S, Lenfant AM, Benaud C, Hartung T, Cecchelli R, Prieto P, Dehouck MP. Induction of blood-brain barrier properties in cultured brain capillary endothelial cells: comparison between primary glial cells and C6 cell line. Glia. 2005; 51:187–198. [PubMed: 15800928]
3. Bowman PD, Ennis SR, Rarey KE, Betz AL, Goldstein GW. Brain microvessel endothelial cells in tissue culture: a model for study of blood-brain barrier permeability. Ann. Neurol. 1983; 14:396–402. [PubMed: 6638956]
4. Braeckmans K, Peeters L, Sanders NN, De Smedt SC, Demeester J. Three-dimensional fluorescence recovery after photobleaching with the confocal scanning laser microscope. Biophys. J. 2003; 85:2240–2252. [PubMed: 14507689]
5. Braga J, Desterro JM, Carmo-Fonseca M. Intra-cellular macromolecular mobility measured by fluorescence recovery after photobleaching with confocal laser scanning microscopes. Mol. Biol. Cell. 2004; 15:4749–4760. [PubMed: 15292455]
6. Brown RC, Morris AP, O'Neil RG. Tight junction protein expression and barrier properties of immortalized mouse brain microvessel endothelial cells. Brain Res. 2007; 1130:17–30. [PubMed: 17169347]
7. Cancel LM, Fitting A, Tarbell JM. In vitro study of LDL transport under pressurized (convective) conditions. Am. J. Physiol. Heart Circ. Physiol. 2007; 293:H126–H132. [PubMed: 17322415]
8. Cancel LM, Tarbell JM. The role of apoptosis in LDL transport through cultured endothelial cell monolayers. Atherosclerosis. 2010; 208:335–341. [PubMed: 19709659]
9. Crone C, Olesen SP. Electrical resistance of brain microvascular endothelium. Brain Res. 1982; 241:49–55. [PubMed: 6980688]
10. Cucullo L, McAllister MS, Kight K, Krizanac-Bengez L, Marroni M, Mayberg MR, Stanness KA, Janigro D. A new dynamic in vitro model for the multidimensional study of astrocyte-endothelial cell interactions at the blood-brain barrier. Brain Res. 2002; 951:243–254. [PubMed: 12270503]

11. Deli MA, Abraham CS, Kataoka Y, Niwa M. Permeability studies on in vitro blood-brain barrier models: physiology, pathology, and pharmacology. Cell. Mol. Neurobiol. 2005; 25:59–127. [PubMed: 15962509]
12. de Vries HE, BlomRoosemalen MCM, van Oosten M, deBoer AG, van Berkel TJC, Breimer DD, Kuiper J. The influence of cytokines on the integrity of the blood-brain barrier in vitro. J. Neuroimmunol. 1996; 64:37–43. [PubMed: 8598388]
13. Engvall E. Structure and function of basement membranes. Int. J. Dev. Biol. 1995; 39:781–787. [PubMed: 8645562]
14. Fletcher NF, Brayden DJ, Brankin B, Worrall S, Callanan JJ. Growth and characterisation of a cell culture model of the feline blood-brain barrier. Vet. Immunol. Immunopathol. 2006; 109:233–244. [PubMed: 16182376]
15. Fraser PA, Dallas AD, Davies S, Fraser PA. Measurement of filtration coefficient in single cerebral microvessels of the frog. J. Physiol. Lond. 1990; 423:343–361. [PubMed: 2388154]
16. Gaillard PJ, de Boer AG. Relationship between permeability status of the blood-brain barrier and in vitro permeability coefficient of a drug. Eur. J. Pharm. Sci. 2000; 12:95–102. [PubMed: 11102736]
17. Gumbleton M, Audus KL. Progress and limitations in the use of in vitro cell cultures to serve as a permeability screen for the blood-brain barrier. J. Pharm. Sci. 2001; 90:1681–1698. [PubMed: 11745727]
18. Hamm S, Dehouck B, Kraus J, Wolburg-Buchholz K, Wolburg H, Risau W, Cecchelli R, Engelhardt B, Dehouck MP. Astrocyte mediated modulation of blood-brain barrier permeability does not correlate with a loss of tight junction proteins from the cellular contacts. Cell Tissue Res. 2004; 315:157–166. [PubMed: 14615934]
19. Haseloff RF, Blasig IE, Bauer HC, Bauer H. In search of the astrocytic factor(s) modulating blood-brain barrier functions in brain capillary endothelial cells in vitro. Cell. Mol. Neurobiol. 2005; 25:25–39. [PubMed: 15962507]
20. Hawkins BT, Davis TP. The blood-brain barrier/ neurovascular unit in health and disease. Pharmacol. Rev. 2005; 57:173–185. [PubMed: 15914466]
21. Hurwitz AA, Berman JW, Rashbaum WK, Lyman WD. Human fetal astrocytes induce the expression of blood-brain barrier specific proteins by autologous endothelial cells. Brain Res. 1993; 625:238–243. [PubMed: 7903899]
22. Johnston H, Baker PJ, Abel M, Charlton HM, Jackson G, Fleming L, Kumar TR, O'Shaughnessy PJ. Regulation of Sertoli cell number and activity by follicle-stimulating hormone and androgen during postnatal development in the mouse. Endocrinology. 2004; 145:318–329. [PubMed: 14551232]
23. Karyekar CS, Fasano A, Raje S, Lu RL, Dowling TC, Eddington ND. Zonula occludens toxin increases the permeability of molecular weight markers and chemotherapeutic agents across the bovine brain microvessel endothelial cells. J. Pharm. Sci. 2003; 92:414–423. [PubMed: 12532391]
24. Kemper EM, Boogerd W, Thuis I, Beijnen JH, van Tellingen O. Modulation of the blood-brain barrier in oncology: Therapeutic opportunities for the treatment of brain tumours? Cancer Treat. Rev. 2004; 30:415–423. [PubMed: 15245774]
25. Kleinman HK, Martin GR. Matrigel: basement membrane matrix with biological activity. Semin. Cancer Biol. 2005; 15:378–386. [PubMed: 15975825]
26. Koto T, Takubo K, Ishida S, Shinoda H, Inoue M, Tsubota K, Okada Y, Ikeda E. Hypoxia disrupts the barrier function of neural blood vessels through changes in the expression of claudin-5 in endothelial cells. Am. J. Pathol. 2007; 170:1389–1397. [PubMed: 17392177]
27. Kraus J, Voigt K, Schuller AM, Scholz M, Kim KS, Schilling M, Schabitz WR, Oschmann P, Engelhardt B. Interferon-beta stabilizes barrier characteristics of the blood-brain barrier in four different species in vitro. Mult. Scler. 2008; 14:843–852. [PubMed: 18505778]
28. Lawrence JR, Wolfaardt GM, Korber DR. Determination of diffusion coefficients in biofilms by confocal laser microscopy. Appl. Environ. Microbiol. 1994; 60:1166–1173. [PubMed: 16349228]
29. LeBleu VS, Macdonald B, Kalluri R. Structure and function of basement membranes. Exp. Biol. Med. (Maywood, N.J.). 2007; 232:1121–1129.

30. Leblond CP, Inoue S. Structure, composition, and assembly of basement membrane. Am. J. Anat. 1989; 185:367–390. [PubMed: 2675590]
31. Lee SW, Kim WJ, Park JA, Choi YK, Kwon YW, Kim KW. Blood-brain barrier interfaces and brain tumors. Arch. Pharm. Res. 2006; 29:265–275. [PubMed: 16681030]
32. Malina KC, Cooper I, Teichberg VI. Closing the gap between the in-vivo and in-vitro blood-brain barrier tightness. Brain Res. 2009; 1284:12–21. [PubMed: 19501061]
33. Michel CC, Curry FE. Microvascular permeability. Physiol. Rev. 1999; 79:703–761. [PubMed: 10390517]
34. Miosge N. The ultrastructural composition of basement membranes in vivo. Histol. Histopathol. 2001; 16:1239–1248. [PubMed: 11642743]
35. Nicolazzo JA, Charman SA, Charman WN. Methods to assess drug permeability across the blood-brain barrier. J. Pharm. Pharmacol. 2006; 58:281–293. [PubMed: 16536894]
36. Omidi Y, Campbell L, Barar J, Connell D, Akhtar S, Gumbleton M. Evaluation of the immortalised mouse brain capillary endothelial cell line, b.End3, as an in vitro blood-brain barrier model for drug uptake and transport studies. Brain Res. 2003; 990:95–112. [PubMed: 14568334]
37. Pardridge WM. Blood-brain barrier biology and methodology. J. Neurovirol. 1999; 5:556–569. [PubMed: 10602397]
38. Poller B, Gutmann H, Krahenbuhl S, Weksler B, Romero I, Couraud PO, Tuffin G, Drewe J, Huwyler J. The human brain endothelial cell line hCMEC/ D3 as a human blood-brain barrier model for drug transport studies. J. Neurochem. 2008; 107:1358–1368. [PubMed: 19013850]
39. Sahagun G, Moore SA, Hart MN. Permeability of neutral vs. anionic dextrans in cultured brain microvascular endothelium. Am. J. Physiol. 1990; 259:H162–H166. [PubMed: 1695819]
40. Salvetti F, Cecchetti P, Janigro D, Lucacchini A, Benzi L, Martini C. Insulin permeability across an in vitro dynamic model of endothelium. Pharm. Res. 2002; 19:445–450. [PubMed: 12033378]
41. Santaguida S, Janigro D, Hossain M, Oby E, Rapp E, Cucullo L. Side by side comparison between dynamic versus static models of blood-brain barrier in vitro: a permeability study. Brain Res. 2006; 1109:1–13. [PubMed: 16857178]
42. Shi ZD, Ji XY, Berardi DE, Qazi H, Tarbell JM. Interstitial flow induces MMP-1 expression and vascular SMC migration in collagen I gels via an ERK1/ 2-dependent and c-Jun-mediated mechanism. Am.J.Physiol. Heart Circ. Physiol. 2010; 298:H127–H135. [PubMed: 19880665]
43. Soga N, Connolly JO, Chellaiah M, Kawamura J, Hruska KA. Rac regulates vascular endothelial growth factor stimulated motility. Cell Commun. Adhes. 2001; 8:1–13. [PubMed: 11775025]
44. Sugaya R, Wolf BA, Kita R. Thermal diffusion of dextran in aqueous solutions in the absence and the presence of urea. Biomacromolecules. 2006; 7:435–440. [PubMed: 16471913]
45. Thompson SE, Cavitt J, Audus KL. Leucine-enkephalin effects on paracellular and transcellular permeation pathways across brain microvessel endothelial-cell monolayers. J. Cardiovasc. Pharmacol. 1994; 24:818–825. [PubMed: 7532761]
46. Tyagi N, Moshal KS, Sen U, Vacek TP, Kumar M, Hughes WM Jr, Kundu S, Tyagi SC. H2S protects against methionine-induced oxidative stress in brain endothelial cells. Antioxid. Redox Signal. 2009; 11:25–33. [PubMed: 18837652]
47. Wang H, Yan SY, Chai H, Riha GM, Li M, Yao QZ, Chen CY. Shear stress induces endothelial transdifferentiation from mouse smooth muscle cells. Bio-chem. Biophys. Res. Commun. 2006; 346:860–865.
48. Wang RS, Yeh S, Chen LM, Lin HY, Zhang CX, Ni J, Wu CC, di Sant'Agnese PA, DeMesy-Bentley KL, Tzeng CR, Chang CS. Androgen receptor in sertoli cell is essential for germ cell nursery and junctional complex formation in mouse testes. Endocrinology. 2006; 147:5624–5633. [PubMed: 16973730]
49. Yamamoto K, Sokabe T, Watabe T, Miyazono K, Yamashita JK, Obi S, Ohura N, Matsushita A, Kamiya A, Ando J. Fluid shear stress induces differentiation of Flk-1-positive embryonic stem cells into vascular endothelial cells in vitro. Am. J. Physiol. Heart Circ. Physiol. 2005; 288:H1915–H1924. [PubMed: 15576436]
50. Yoder EJ. Modifications in astrocyte morphology and calcium signaling induced by a brain capillary endothelial cell line. Glia. 2002; 38:137–145. [PubMed: 11948807]

51. Yuan W, Li G, Fu BM. Effect of surface charge of immortalized mouse cerebral endothelial cell monolayer on transport of charged solutes. Ann. Biomed. Eng. 2010 Jan 20. Epub ahead of print.PMID: 20087768.

52. Yuan W, Lv Y, Zeng M, Fu BM. Non-invasive measurement of solute permeability in cerebral microvessels of the rat. Microvasc. Res. 2009; 77:166–173. [PubMed: 18838082]

53. Zhang Y, Li CSW, Ye YY, Johnson K, Poe J, Johnson S, Bobrowski W, Garrido R, Madhu C. Porcine brain microvessel endothelial cells as an in vitro model to predict in vivo blood-brain barrier permeability. Drug Metab. Dispos. 2006; 34:1935–1943. [PubMed: 16896068]

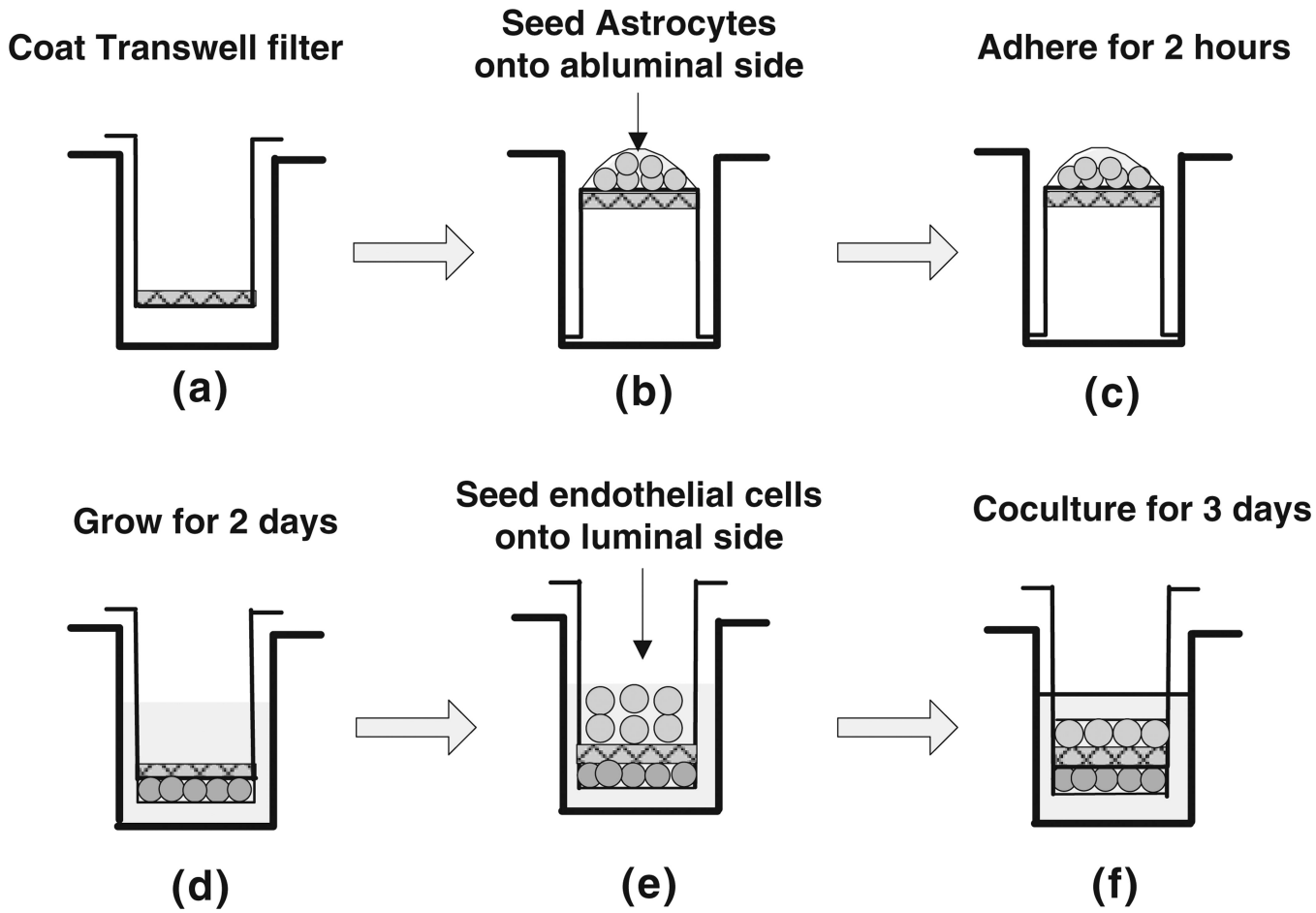

FIGURE 1.

The experimental procedure for coculturing the bEnd3 cells and astrocytes on different sides of the Transwell filter with 0.4 μm diameter pores. The Transwell filter consists of a porous membrane support submerged in culture medium. The Transwell filters were coated with fibronectin or basement membrane substitute (a). Astrocytes were first seeded onto the abluminal side of the inverted Transwell filter at a density of 2.75×10^4 cells per filter (b), allowed to adhere for 2 h (c), then the filter was flipped back and the astrocytes were cultured for 2 days in DMEM supplemented with 10% FBS and 1% PS (d). At the end of the second day, bEnd3 cells were seeded onto the luminal side of Transwell filter at a density of 6.6×10^4 cells per filter (e) and cocultured with astrocytes for an additional 3–4 days (f). The culture medium for the bEnd3 cells on the luminal side of the Transwell filter was DMEM supplemented with 10% FBS, 1% PS and 3 mM L-Glutamine.

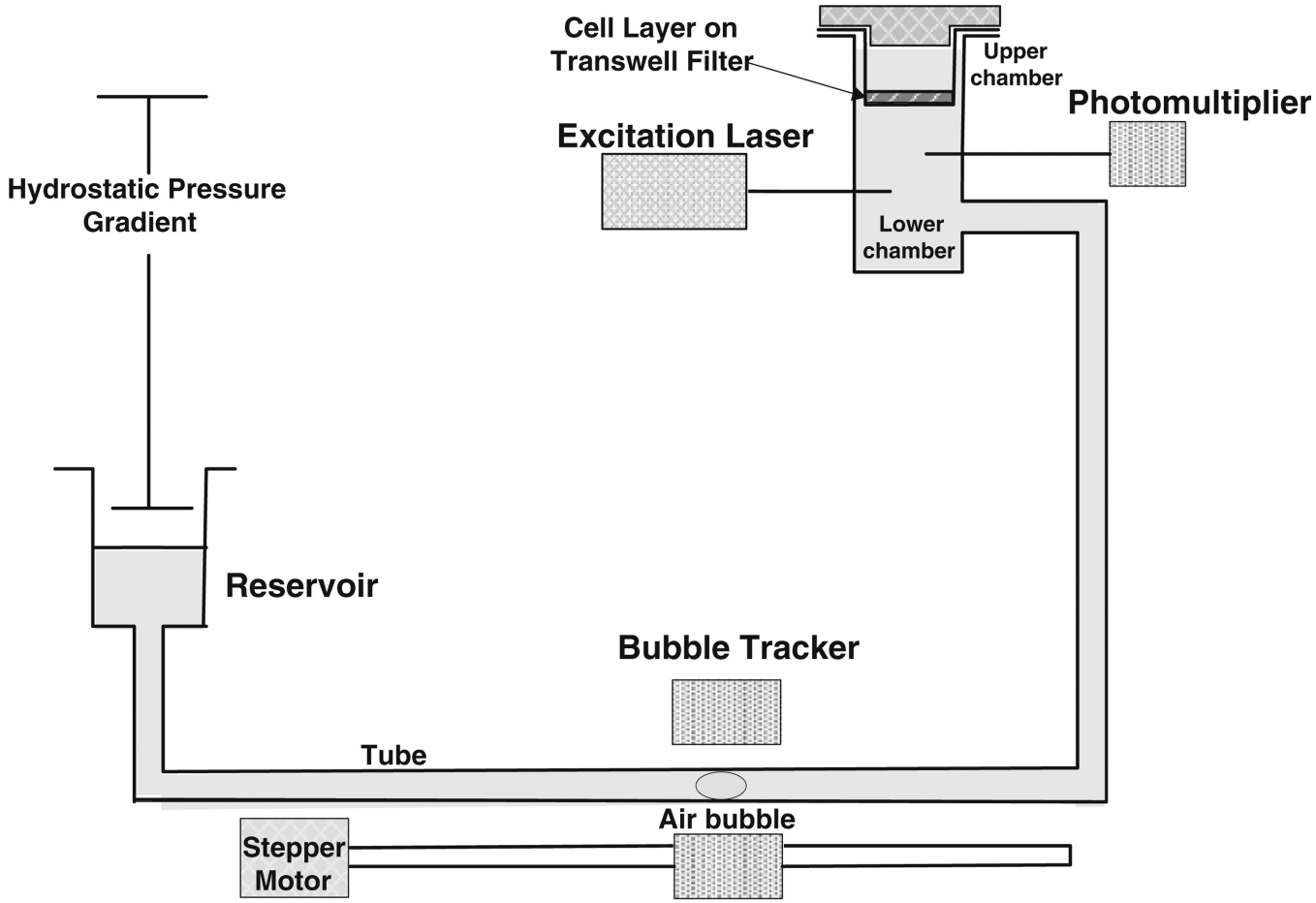

FIGURE 2.

Schematic of the experimental system used to measure the permeability of the *in vitro* BBB models to water and fluorescently-labeled solutes. The Transwell filter with the cell layers was sealed in a chamber. For solute transport, the fluorescently-labeled test solute was added to the upper chamber, transport of test solutes across the cell layer was quantified by an automated fluorometer and the solute permeability was calculated accordingly. For water transport, the reservoir was lowered to create a pressure gradient across the cell layer, the water flux across the cell monolayer was measured by a bubble tracker, and the hydraulic conductivity was determined accordingly.

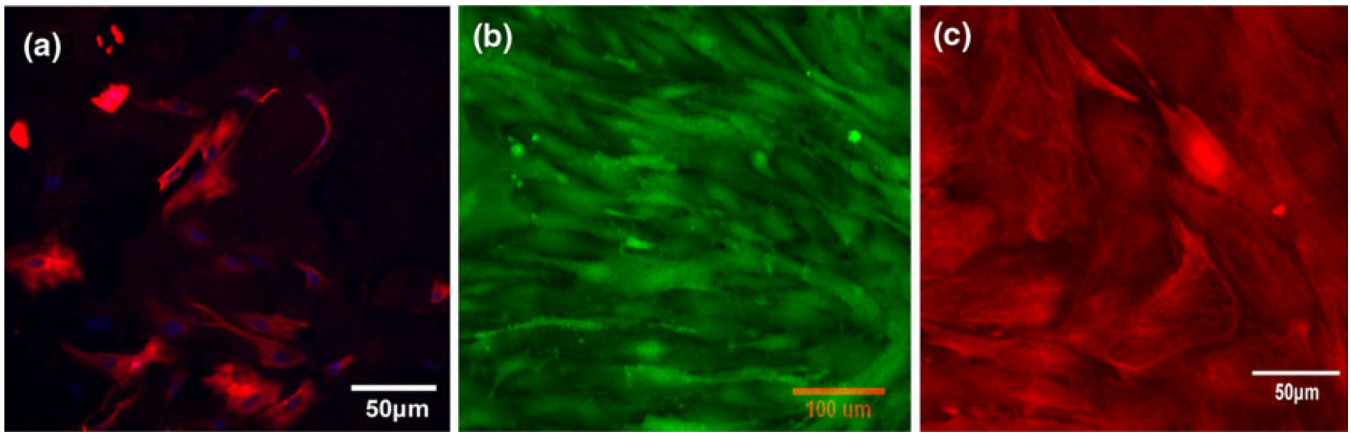

FIGURE 3.

Immunostaining results for astroyctes (a) Astrocytes immunolabeled with antibodies against glial fibrillary acidic protein (GFAP, *red*) and counterstained with cell nucleus dye DAPI (*blue*). Primary astrocytes (passage P3–P5) were seeded on the luminal side of the Transwell filter at a density of 5.5×10^3 cells per filter and cultured for 3 days before immunostaining. The purity of isolated astrocytes was >90%. (b) Cytoplasmic labeling (*green*) of the astrocyte monoculture by Calcein AM. Astrocytes were seeded onto the luminal side of the Transwell filter at a seeding density of 2.75×10^4 cells per filter and grown for 5 days, forming a confluent monolayer on the luminal side of the Transwell filter which was used to perform the permeability measurement. (c) Labeling of GFAP (*red*) in astrocytes when cocultured with bEnd3 cells at the end of 5th day.

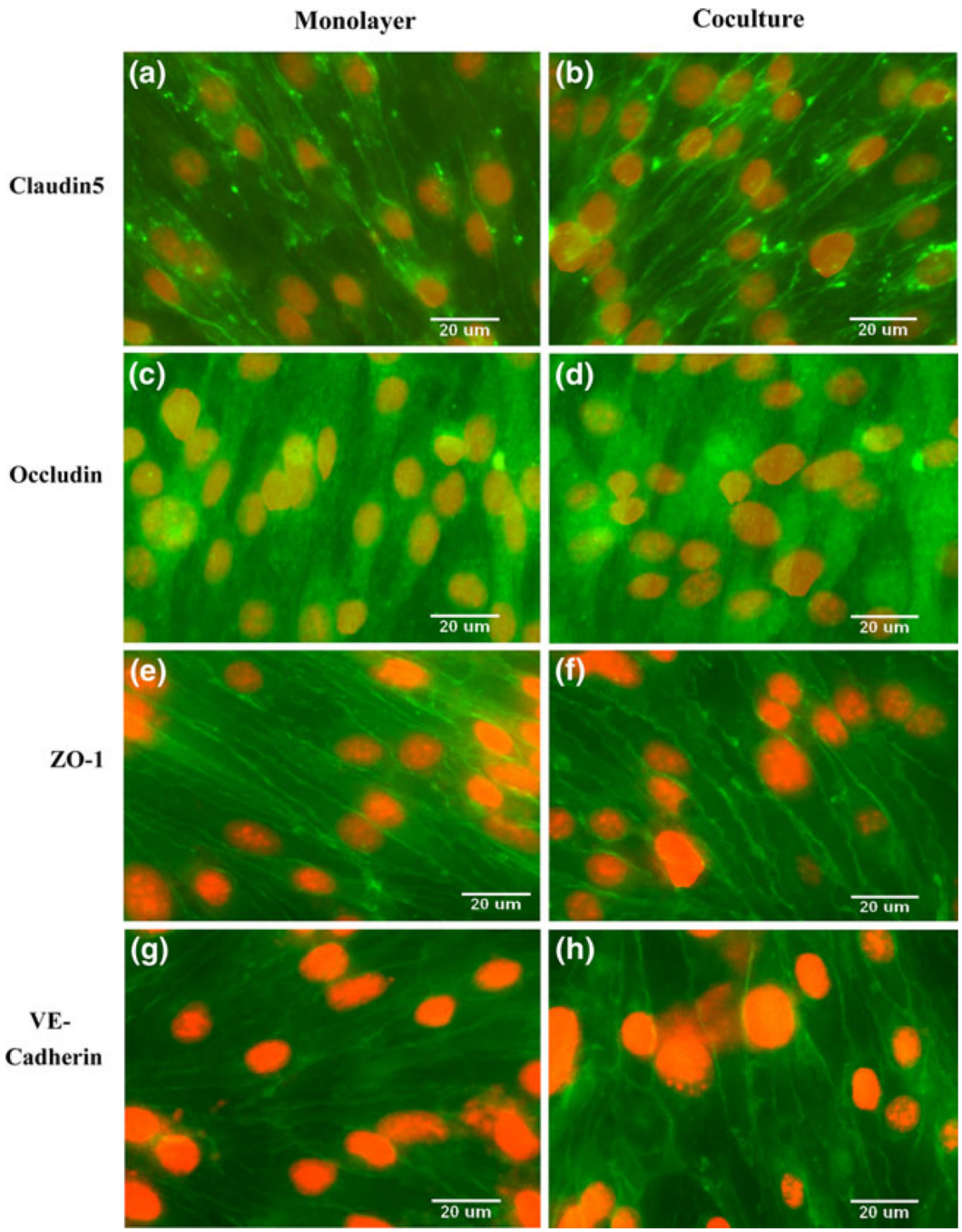

FIGURE 4.

Comparison of essential junction proteins expressed by bEnd3 cells when cultured alone (*left panel*) or cocultured with astrocytes (*right panel*). Immunostaining of claudin-5 (a, b); occludin (c, d); ZO-1 (e, f); and VE-cadherin (g, h). Endothelial cells were seeded to the luminal side of the Transwell filter with a density of 6.6×10^4 cells per filter and cultured for 3–4 days in DMEM supplemented with 10% FBS, 1% PS and 3 mM Glutamine (*left panel*). Astrocytes were seeded onto the abluminal side with a density of 2.75×10^4 cells per

filter two days before endothelial cell seeding and then cultured in DMEM supplemented with 10% FBS for an additional 3–4 days (*right panel*).

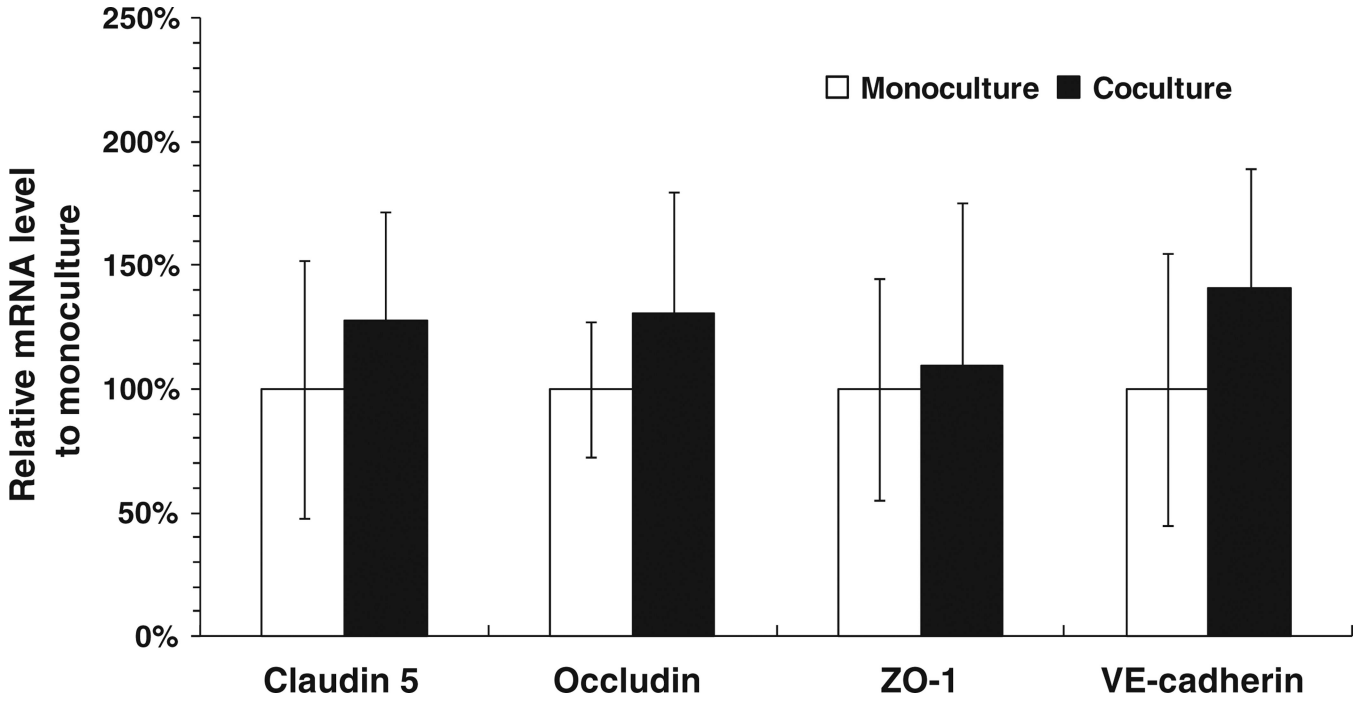

FIGURE 5.

Comparison of gene expressions of bEnd3 cells by RT-qPCR when cultured alone (*empty bars*) and cocultured with astrocytes (*filled bars*) for claudin-5, occludin, ZO-1, VE-cadherin. Data shown in mean ± SD (n = 3).

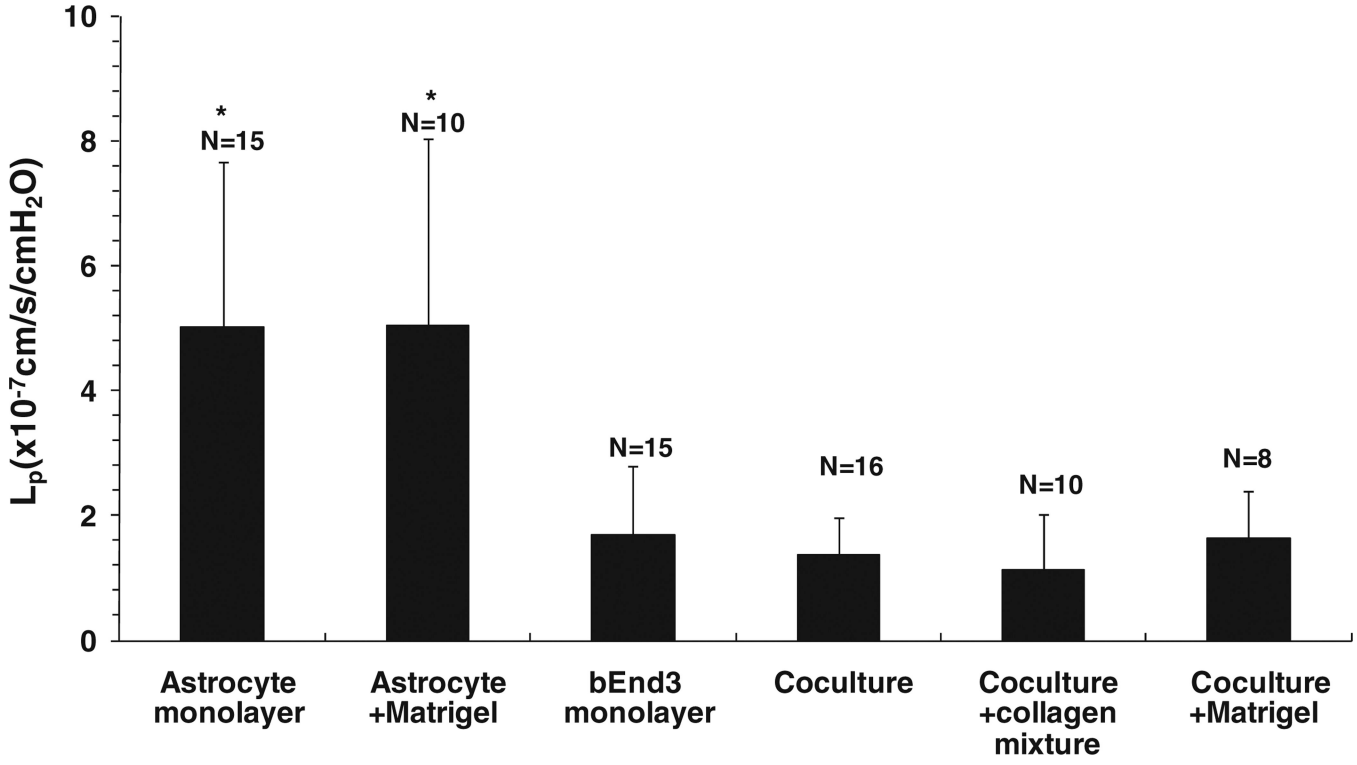

FIGURE 6.

Hydraulic conductivity (L_p) of the *in vitro* BBB models: astrocyte monoculture, astrocyte monoculture on top of a thin Matrigel coating (Astrocyte + Matrigel), bEnd3 monoculture, coculture of astrocytes and bEnd3 cells on different sides of a Transwell filter (coculture), coculture with a thin coating of a mixture of collagen types I and IV on the luminal side of a Transwell filter (coculture + collagen mixture), coculture with a thin Matrigel coating on the abluminal side of a Transwell filter (coculture + Matrigel). The values are presented as mean ± SD. * $p < 0.05$ compared to bEnd3 monolayer.

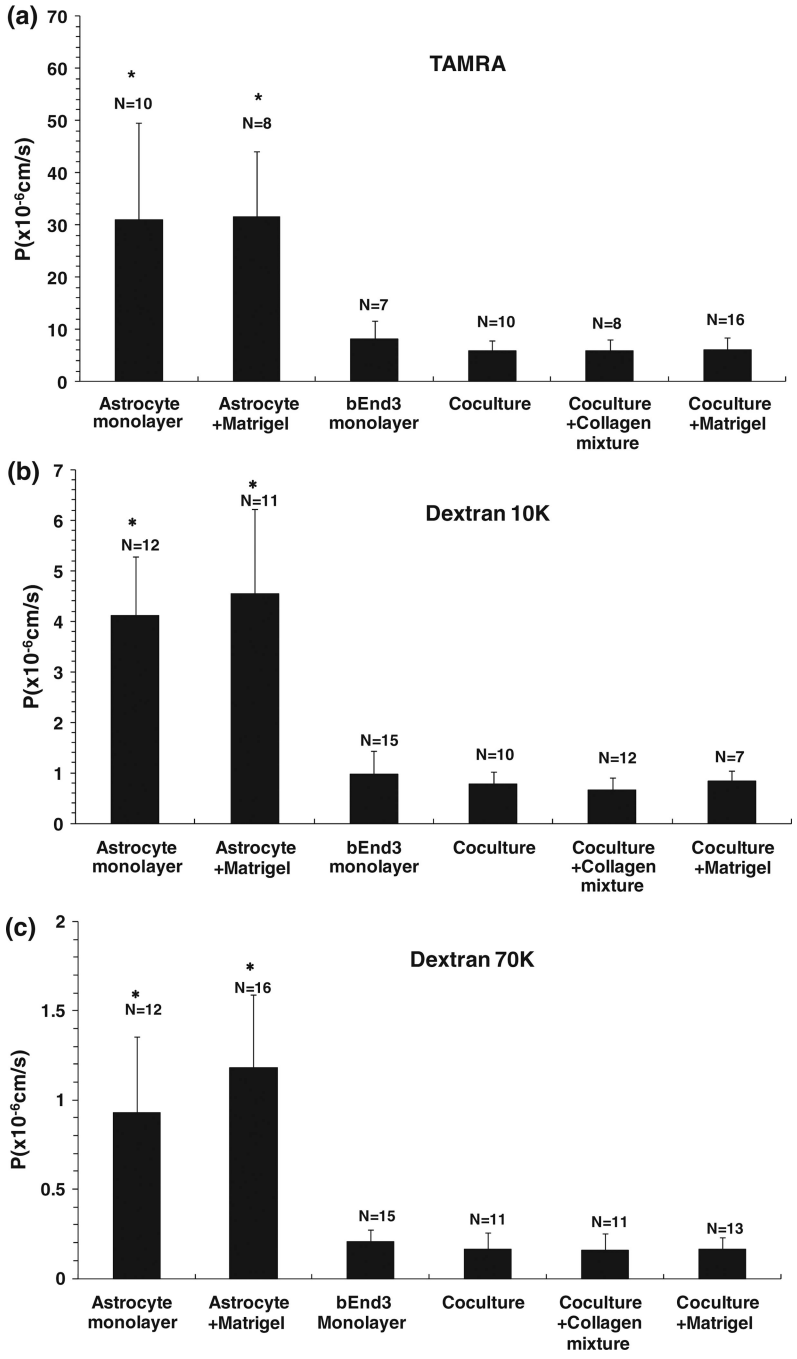

FIGURE 7.

Diffusive permeability (*P*) of the *in vitro* BBB models to three solutes: (a) Tetramethyl-6-Carboxyrhodamine (TAMRA) (MW = 467); (b) Dextran 10K; (c) Dextran 70K. The definitions for the *in vitro* BBB models are the same as in Fig. 6. The values are presented as mean ± SD. * $p < 0.01$ compared to bEnd3 monolayer.

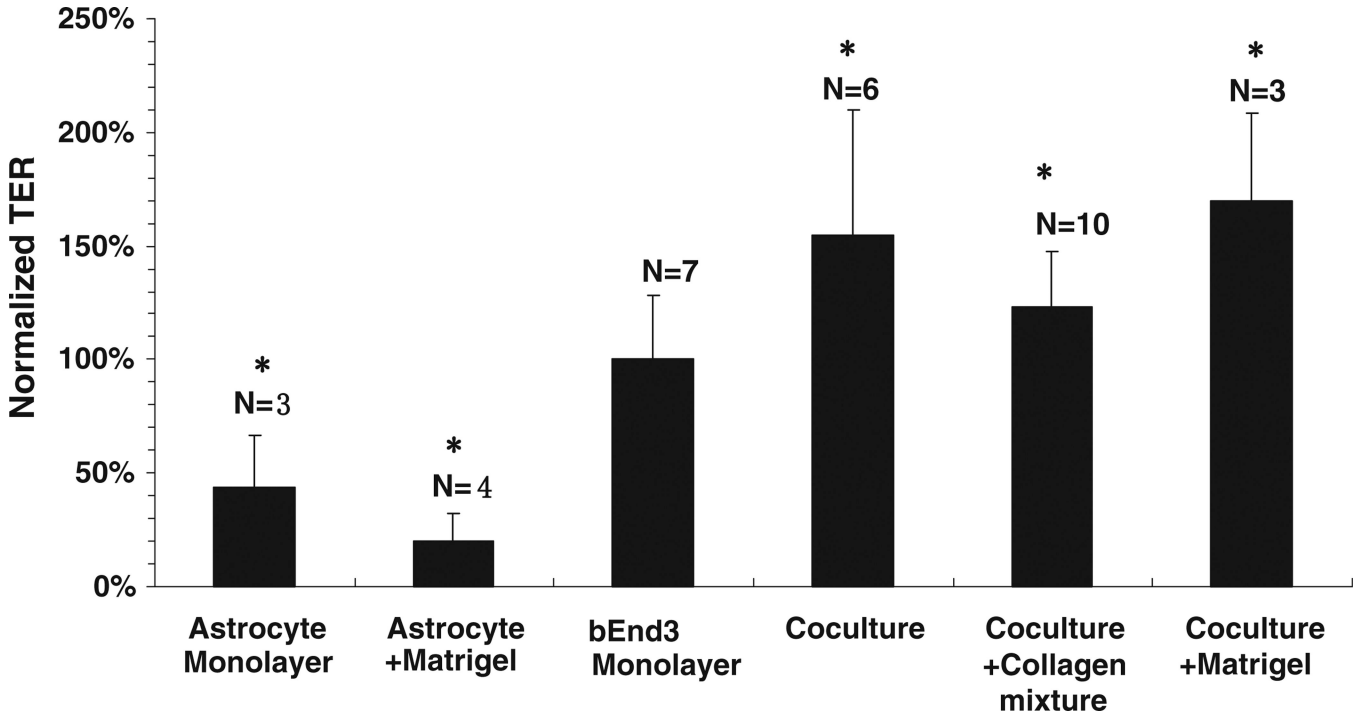

FIGURE 8.

The ratio of the transendothelial electrical resistance (TER) of different *in vitro* BBB models to that of the bEnd3 monolayer. The abbreviations for the *in vitro* BBB models are the same as in Fig. 6. The values are presented as mean ± SD. * $p < 0.02$ compared to bEnd3 monolayer.

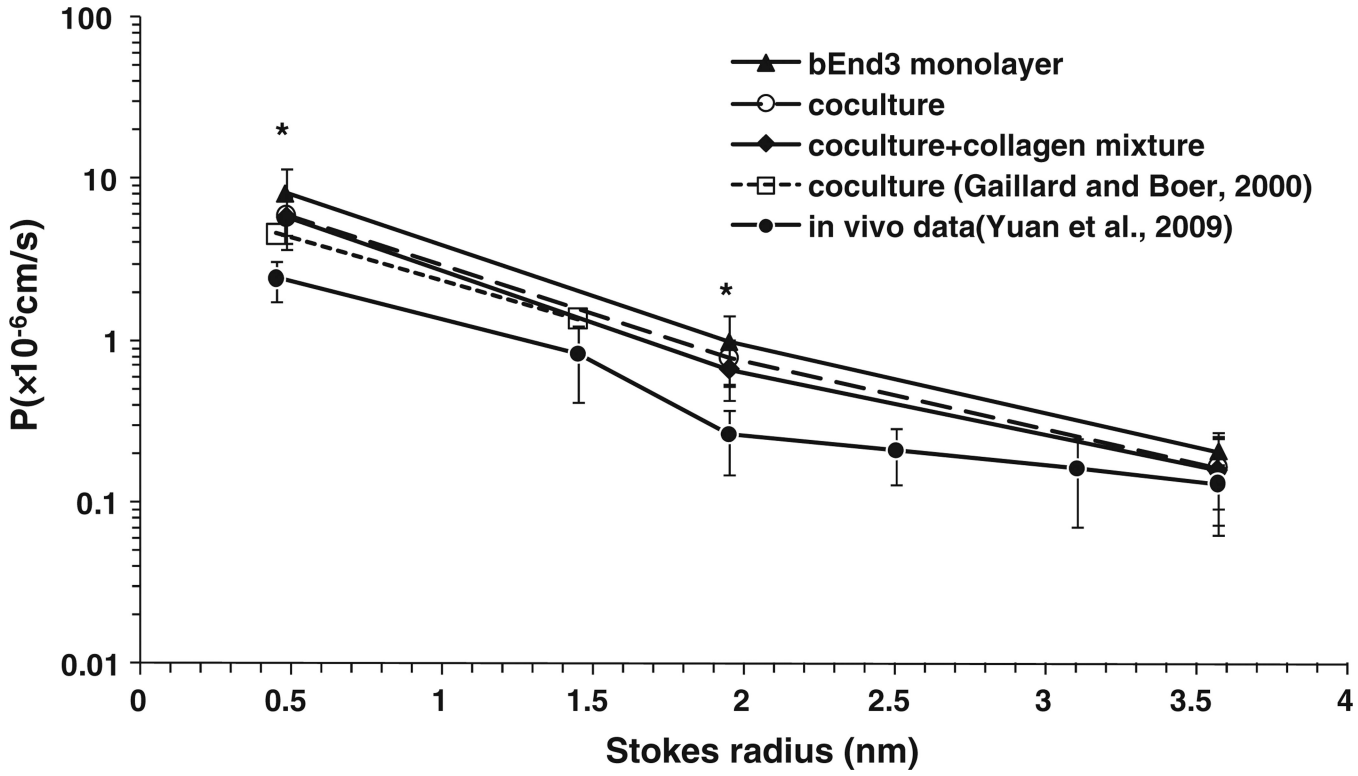

FIGURE 9.

Comparison of diffusive permeability *P* of the bEnd3 monoculture, coculture, and coculture with collagen mixture with *in vivo* data from rat pial microvessels in Yuan *et al.*[52] and that from a coculture model in Gaillard and Boer.[16] The values are presented as mean ± SD. * $p < 0.005$ compared to corresponding *in vivo* data.

TABLE 1

Real-time PCR primers for junction proteins.

Protein	Accession number	Forward primer (5’ to 3’)	Reverse primer (5’ to 3’)	Reference
Claudin 5	NM_ 013805	TAA GGC ACG GGT AGC ACT CA	GCC CAG CTC GTA CTT CTG TG	
Occludin	NM_ 008756.2	ATC CTG TCT ATG CTC ATT ATT GTG	CTG CTC TTG GGT CTG TAT ATC C	Wang *et al.*[48]
VE-cadherin	X83930	TCC TCT GCA TCC TCA CTA TCA CA	GTA AGT GAC CAA CTG CTC GTG AAT	Wang *et al.*[47]
ZO-1	NM_009386.2	GGA GCT ACG CTT GCC ACA CT	GGT CAA TCA GGA CAG AAA CAC AGT	Johnston *et al.*[22]
β-Actin	NM_007393.2	GTC GTA CCA CAG GCA TTG TGA TGG	GCA ATG CCT GGG TGC ATG GTG G	Yamamoto *et al.*[49]